Dalton
Transactions

Cite this: *Dalton Trans.*, 2012, **41**, 12898

www.rsc.org/dalton

PAPER

Convenient synthesis of fluoride-alkoxides of Nb(v) and Ta(v): a spectroscopic, crystallographic and computational study†

Marco Bortoluzzi,[a] Nicola Guazzelli,[b] Fabio Marchetti,*[b] Guido Pampaloni[b] and Stefano Zacchini[c]

Received 11th April 2012, Accepted 28th August 2012
DOI: 10.1039/c2dt31453c

The synthesis and the spectroscopic characterization of fluoride-alkoxides of niobium and tantalum in the highest oxidation state are reported. Suspensions of MF_5 (M = Nb, Ta) in a chlorinated solvent reacted with up to three equivalents of $ROSiMe_3$ (R = Me, Et, Ph) to afford polynuclear derivatives and variable amounts of $FSiMe_3$. Thus $MF_4(OR)$ (R = Et, Ph) and $MF_3(OR)_2$ were obtained by selective 1 : 1 and 1 : 2 reactions almost exclusively as single isomeric products; otherwise mixtures of $MF_4(OMe)$ species were afforded from the equimolar reactions of MF_5 with $MeOSiMe_3$. The 1 : 3 reaction of TaF_5 with $MeOSiMe_3$ led to different forms of $TaF_2(OMe)_3$. The synthesis of $TaF(OPh)_4$ was forced by high temperature conditions or the use of a large excess of $PhOSiMe_3$. DFT studies were carried out in order to predict, in the distinct cases, the most stable structures of the metal products. The molecular structures of $[NbF_2(OPh)_2(\mu\text{-}F)]_3$ and $[TaF(OPh)_3(\mu\text{-}OPh)]_2$ were ascertained by X-ray diffraction.

Introduction

In the last few years there has been increasing development in the chemistry of niobium and tantalum derivatives, encouraged by the easy availability and the substantial non-toxicity of the metals.[1]

In this context the alkoxides/aryloxides of Nb(v) and Ta(v) have found interesting applications in catalysis[1a,2] and as precursors of the corresponding oxides,[3] which in turn have remarkable electrical and optical properties.[4]

Both the pentaalkoxide species $M(OR)_5$ (M = Nb, Ta; R = alkyl or aryl)[2a,3a,5] and the mixed halide-alkoxides $MX_n(OR)_{5-n}$ (X = Cl or Br, n = 1–3)[6] are well-known compounds, which typically adopt a dinuclear structure with two ligands bridging between the two metal centres. On the other hand, very little is known on the corresponding fluoride-alkoxides. Mixed fluoride-alkoxides of a variety of metals have been usually prepared by three strategies: (*a*) alkoxide-fluoride exchange by reaction of metal alkoxides with HF,[7,8] KHF_2,[9] PF_3[10] or MeCOF;[11] (*b*) fluoride-alkoxide exchange by reaction of metal fluorides with alcohols; (*c*) metathesis reaction between metal alkoxides and metal fluorides.[12–14] As an example (point *b*), mononuclear complexes $WF_{6-x}(OEt)_x$ (x = 1, 2) have been obtained from WF_6 by treatment with ethanol.[13,15]

Nevertheless, in the case of Nb(v) and Ta(v) this last procedure is not viable for the preparation of $MF_{5-x}(OR)_x$ complexes (M = Nb, Ta), due to the special strength of the M–F bond in MF_5, preventing the fluoride displacement.[1a,16] Otherwise the synthesis of some Nb(v) and Ta(v) fluoride alkoxides (and related coordination adducts[17]) was claimed in the past by metathesis reaction between MF_5 and $M(OR)_5$ (M = Nb, Ta; R = Et, Ph),[18] see point (*c*) above. Nevertheless the characterization of the products was limited and a clear structural determination has been still missing.

The successful competition for fluorine of Si towards Nb was casually demonstrated, when high thermal treatment of NbF_5 in silicon-containing tubes gave SiF_4 and niobium oxy-fluorides.[19] Hence amido-fluorides and chloro-fluorides were prepared by reactions of MF_5 (M = Nb, Ta) with trimethylsilyl species.[20] On considering these facts, we decided to investigate the reactivity of niobium and tantalum pentafluorides, MF_5 (M = Nb, **1a**; M = Ta, **1b**),[21] with trimethylsilyl ethers, $ROSiMe_3$.

The reactions, with different molar ratios, proceeded straightforwardly with both alkyl (R = Me, Et) and aryl (R = Ph) groups, and led to the high-yield formation of fluoride-alkoxide (aryloxide) derivatives. The determination of the structures of the products obtained relied on combined spectroscopic and DFT studies. The two first examples of X-ray characterization of niobium and tantalum fluoride-phenolates will be presented.

Results and discussion

When suspensions of MF_5 (M = Nb, **1a**; M = Ta, **1b**) in dichloromethane were treated with 1–3 molar equivalents of

---

[a] *University of Venezia, Dipartimento di Scienze Molecolari e Nanosistemi, Dorsoduro 2137, I-30123 Venezia, Italy*
[b] *University of Pisa, Dipartimento di Chimica e Chimica Industriale, Via Risorgimento 35, I-56126 Pisa, Italy. E-mail: fabmar@dcci.unipi.it; Fax: +39 050 2219246; Tel: +39 050 2219245*
[c] *University of Bologna, Dipartimento di Chimica Fisica e Inorganica, Viale Risorgimento 4, I-40136 Bologna, Italy*

† Electronic supplementary information (ESI) available. CCDC 876459 (**3eB**) and 876460 (**5A**). For ESI and crystallographic data in CIF or other electronic format see DOI: 10.1039/c2dt31453c

M	R	Compound
	$n = 1$	
Nb	Me	**2a**
Ta	Me	**2b**
Nb	Et	**2c**
Ta	Et	**2d**
Nb	Ph	**2e**
Ta	Ph	**2f**
	$n = 2$	
Nb	Me	**3a**
Ta	Me	**3b**
Nb	Et	**3c**
Ta	Et	**3d**
Nb	Ph	**3e**
Ta	Ph	**3f**
	$n = 3$	
Ta	Me	**4**

Scheme 1 New $MF_{5-n}(OR)_n$ compounds.

trimethylsilyl ethers $ROSiMe_3$ (R = Me, Et, Ph), exothermic dissolution of the solid took place. The metal containing products $MF_4(OR)$ (**2a–f**), $MF_3(OR)_2$ (**3a–f**) and $TaF_2(OMe)_3$ (**4**) could be isolated in pure form upon removal of the volatile materials, see Scheme 1. The compounds **2–4** are solids at 20 °C, apart from $MF_3(OEt)_2$ which appear as viscous liquids. The colours range from colourless to yellow, with the exception of the pale blue $NbF_3(OMe)_2$, probably due to some Nb(IV) impurity. NMR experiments pointed out that the reactions in CD_2Cl_2 proceeded with complete consumption of the organic reagent and clean formation of $FSiMe_3$, according to eqn (1).

$$MF_5 + n\text{ROSiMe}_3 \rightarrow MF_{5-n}(\text{OR})_n + n\text{FSiMe}_3 \qquad (1)$$

NMR samples were prepared respectively by addition of 1, 2 and 3 molar equivalents of $ROSiMe_3$ (R = Me, Et, Ph) to CD_2Cl_2 suspensions of MF_5, at room temperature. Thus the NMR spectra were recorded at low temperature in order to prevent ligand-exchange processes. Furthermore IR analyses were carried out, when possible, on the solid mixtures obtained by the reactions conducted in CH_2Cl_2, after removal of the volatile materials.

Compounds $MF_4(OR)$ (2a–f)

The ^{13}C spectra of $MF_4(OPh)$ at 188 K display one resonance accounting for *ipso*-carbon nuclei (*e.g.* at 159.7 ppm in the case of M = Ta, **2f**). This fact suggests the presence of one single species bearing symmetrically-arranged phenolato ligands. Analogous conclusion may be traced for $MF_4(OEt)$ and $TaF_4(OMe)$, on account of the fact that the ^1H and ^{13}C spectra contain one largely-prevalent set of resonances [*e.g.* for **2d**: $\delta(^1H) = 5.22$, (q, 2 H, CH_2), 1.60 (t, 3 H, CH_3) ppm; $\delta(^{13}C) = 81.6$ (CH_2), 16.7 (CH_3) ppm]. On the other hand, $NbF_4(OMe)$ is obtained in several forms (see Experimental).

The ^{19}F NMR spectra of **2a–f** at room temperature display very broad signals; on lowering the temperature, the signals become progressively more resolved and the integrated ratio between resonances due to terminally-bound fluorines and resonances due to bridging fluorines increases. The ^{19}F spectrum of **2f** at 188 K shows the resonances related to the terminal fluorines in the range 156–85 ppm, and the resonances related to the bridging ones in the range −66 to −84 ppm. It should be noted here that the low-temperature ^{19}F NMR patterns (in CD_2Cl_2) of the anions $[M_2F_{11}]^-$ (M = Nb, Ta) consist of three resonances, *e.g.* at δ = 116 and 71 ppm (terminal-F) and −74 ppm (bridging-F) in the case of $[Ta_2F_{11}]^-$.[16b]

The IR spectra of the mixtures **2a–f** (see Experimental) are helpful in the identification of the structure of the related compounds, indeed they suggest the almost absence of bridging alkoxides. For instance, the IR spectrum of **2c** shows two clear, strong absorptions in the 1000–1100 cm^{-1} region (*i.e.* at 1096 and 1063 cm^{-1}). Since the IR spectrum of $[Nb(OEt)_5]_2$ comprises two C–O bands due to the terminal ligands at 1110 and 1066 cm^{-1} and one C–O band attributed to the bridging ligands at 1030 cm^{-1},[22] it may be concluded by comparison that **2c** does not contain bridging ethoxides.

DFT calculations were carried out with the aim to predict the molecular structures of $[TaF_4(OR)]_n$ (R = Me, **2b**; R = Ph, **2f**). Three nuclearities were considered, *i.e.* n = 4, 3, 2: this appears reasonable since tantalum pentafluorides are tetranuclear[21] while tantalum pentaalkoxides are generally dinuclear in the solid state (see Introduction). Hence a series of plausible isomeric structures, for each nuclearity, were optimized for the gas phase; an implicit solvation model for CH_2Cl_2 was added subsequently. An analogous study was carried out on $TaF_4(OEt)$ (**2d**), by considering a restricted series of possibilities. The structures calculated for **2b,d,f** and the related energies are represented respectively in Fig. S1–S4 (**2b**), S5–S8 (**2f**) and S9 (**2d**), within the ESI.†

The most probable structures of **2b,d,f** in dichloromethane are tetranuclear and homologous (respectively **2bN**, **2dN** and **2fN**). However the DFT calculations have indicated that three possible structures of **2b** (*i.e.* **2bJ**, trinuclear; **2bO** and **2bR**, tetranuclear) have energies [referred to the $TaF_4(OMe)$ unit] higher than that of **2bN** by less than 1.5 kcal mol^{-1}, after addition of the solvation model (Fig. S4†). Similar considerations are valid for **2f** (Fig. S8†). The ground-state energy values of dinuclear species are significantly higher in the case of both **2b** and **2f** (Fig. S4 and S8†). The same stability scale (dinuclear ≪ trinuclear < tetranuclear) has been found for the ethoxy-derivative $TaF_4(OEt)$ (**2d**), see Fig. S9.†

The four lowest-energy structures calculated for **2b** are shown in Fig. 1.

The DFT outcomes regarding the tantalum complexes **2b,d,f** may be extended to the corresponding niobium ones (**2a,c,e**). In fact the NMR patterns of **2a,c,e** resemble those of **2b,d,f**, respectively. In addition, we have recently demonstrated thoroughly that the identity of the metal does not play a perceptible role in the chemistry of MF_5 (M = Nb, Ta) and their derivatives.[1a]

The presumed prevalent formation of tetranuclear species in the course of the 1 : 1 reactions of MF_5 with $ROSiMe_3$ is in accord with previous hypothesis on the nuclearity of $NbF_4(OEt)$, based on cryoscopy in benzene.[18a]

However the theoretical existence of different forms of comparable energies, bearing tetra- or trinuclear structure, may explain the formation of more than one product. According to this, the NMR spectra of **2a,b,d** at low temperature display more than one set of resonances; for instance, the ^1H spectrum of **2a**

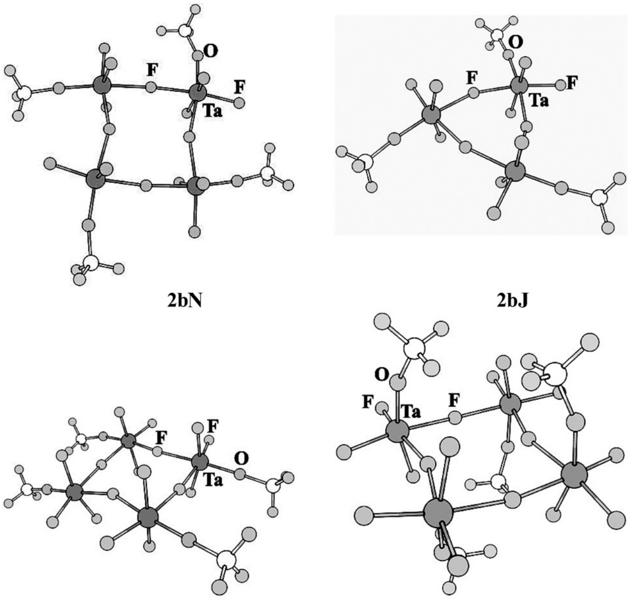
2bN 2bJ

2bR 2bO

Fig. 1 Lowest-energy DFT-optimized structures of $TaF_4(OMe)$.

shows singlets at δ 4.69, 4.59, 4.49, 3.93, 3.84 ppm, in an 8 : 6 : 4 : 1 : 2 ratio (see Experimental). Otherwise the NMR spectra of **2c,e,f** show single sets of resonances, thus suggesting the formation, in each case, of a unique product form. The ^1H NMR spectrum of a $CDCl_3$ solution obtained by 1 : 1 reaction of NbF_5 with $EtOSiMe_3$ did not show variations after prolonged heating at high temperature.

An important point of agreement between the DFT outcomes and the spectroscopic features (NMR and IR, see above) is given by the fact that the lowest energy structures calculated for **2** show symmetrically-distributed terminal –OR ligands [see Fig. 1 for $TaF_4(OMe)$].

In view of the tetranuclear structure of TaF_5, the reactions leading to **2a–f** might proceed with initial formation of intermediates of formula $M_4F_{19}(OR)$. According to DFT calculations, the most stable $Ta_4F_{19}(OMe)$ molecule holds the methoxy group in the equatorial-terminal position (see Fig. S10†). The further multiple substitution of fluorides by [OMe] to give **2bN**, in CH_2Cl_2, is a strongly exothermic process (see eqn (2)).

$$Ta_4F_{19}(OMe) + 3\ MeOSiMe_3 \rightarrow [TaF_4(OMe)]_4 + 3\ FSiMe_3 \quad \Delta H_{calc} = -44\ \text{kcal mol}^{-1} \tag{2}$$

This outcome suggests that partially substituted products are probably not obtained when the reaction of MF_5 with $ROSiMe_3$ is performed with a M/Si = 1 ratio.

Compounds $MF_3(OR)_2$ (3a–f)

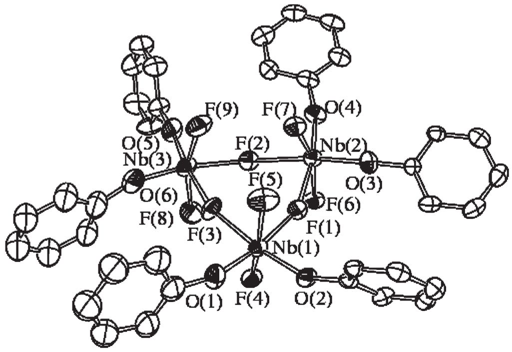

Fig. 2 Molecular structure of $[NbF_2(\mu\text{-}F)(OPh)_2]_3$, **3eB**, with key atoms labelled. The H-atoms have been omitted for clarity. Thermal ellipsoids are at the 50% probability level.

Table 1 Selected bond distances (Å) and angles (°) for **3eB**

Nb(1)–O(1)	1.808(6)	Nb(1)–O(2)	1.835(5)
Nb(1)–F(1)	2.073(5)	Nb(1)–F(3)	2.071(4)
Nb(1)–F(4)	1.873(5)	Nb(1)–F(5)	1.879(5)
Nb(2)–O(3)	1.829(5)	Nb(2)–O(4)	1.822(5)
Nb(2)–F(1)	2.083(4)	Nb(2)–F(2)	2.091(4)
Nb(2)–F(6)	1.898(4)	Nb(2)–F(7)	1.878(5)
Nb(3)–O(5)	1.815(6)	Nb(3)–O(6)	1.827(6)
Nb(3)–F(2)	2.070(5)	Nb(3)–F(3)	2.075(5)
Nb(3)–F(8)	1.882(5)	Nb(3)–F(9)	1.870(5)
F(3)–Nb(1)–F(1)	81.69(18)	F(1)–Nb(2)–F(2)	80.65(17)
F(2)–Nb(3)–F(3)	81.35(18)	Nb(1)–F(1)–Nb(2)	155.9(2)
Nb(3)–F(2)–Nb(2)	153.3(2)	Nb(1)–F(3)–Nb(3)	157.7(3)
F(4)–Nb(1)–F(5)	160.8(2)	F(6)–Nb(2)–F(7)	159.6(2)
F(8)–Nb(3)–F(9)	160.8(2)	O(1)–Nb(1)–O(2)	99.4(3)
O(3)–Nb(2)–O(4)	99.5(3)	O(5)–Nb(3)–O(6)	98.0(3)

X-ray quality crystals of $[NbF_2(\mu\text{-}F)(OPh)_2]_3$ (**3eB**) were collected from a solution obtained by 1 : 2 molar reaction of NbF_5 with $PhOSiMe_3$. Hence the molecular structure could be elucidated by X-ray diffraction: the ORTEP representation is shown in Fig. 2, whereas relevant bond lengths and angles are reported in Table 1.

Compound **3eB** is a cyclic trimer composed of three (distorted) octahedral Nb(V) units bridged by three F-atoms. Each niobium is coordinated to two terminal OPh (in relative *cis*-equatorial positions), two terminal fluorides (in *trans*-axial positions) and two bridging fluorides (lying on the same plane of the phenolato ligands). As far as we are aware, no other $Nb_3(\mu\text{-}F)_3$ species has been known hitherto. For the sake of comparison, it should be cited that NbF_5 in the solid state adopts a tetrameric structure, composed of octahedral units.[23] In the case of **3eB**, the Nb–$F_{terminal}$ interactions [average 1.880(12) Å] are shorter than the bridging contacts [average 2.077(11) Å], as found also in $[NbF_5]_4$ [Nb–$F_{terminal}$ 1.77 Å; Nb–$F_{bridging}$ 2.06 Å]. Nonetheless, it must be remarked that whereas the Nb–$F_{bridging}$ distances in both **3eB** and $[NbF_5]_4$ are almost identical, Nb–$F_{terminal}$ interactions in **3eB** are 0.11 Å longer than in $[NbF_5]_4$. This difference likely originates from the different electronic and steric properties of the ligands present in the two complexes herein described, *i.e.* $[NbF_5]_4$ and **3eB**. The Nb–F–Nb angle [average 155.6(4)°] is considerably bended in view of the trimeric nature of **3eB**, compared to the almost linear Nb–F–Nb interactions [182.5°] found in the tetrameric $[NbF_5]_4$. The Nb–O lengths are in the range of typical niobium–terminal alkoxide interactions.[2a,24]

With the aim to carry out a DFT study on the 1 : 2 reaction of NbF_5 with $PhOSiMe_3$, we considered a series of possible structures of $NbF_3(OPh)_2$. The optimized structures are given in Fig. S11 (ESI†) with the related energies. A solvation model having the dielectric constant of CH_2Cl_2 was included in the calculations.

According to the DFT results, the 1 : 2 reaction of NbF_5 with $PhOSiMe_3$ in CH_2Cl_2 should afford a mixture of products, with slight prevalence of $[NbF_2(\mu\text{-}F)(OPh)_2]_3$ (**3eB**). In fact two additional molecules bearing high symmetry and terminal phenolato ligands (see Fig. S11:† **3eC**, trinuclear; **3eD**, tetranuclear) present energies [referred to the $NbF_3(OPh)_2$ unit] comparable to that of **3eB**.

A selection of calculated geometric parameters for $[NbF_2(\mu\text{-}F)(OPh)_2]_3$ (**3eB**) is supplied within the ESI (Table S1†). A compared reading of Table 1 and Table S1† outlines that the DFT parameters are in satisfying agreement with the experimental data (X-ray). A slight overestimation of bond lengths, typical of most of DFT functionals, is observable.[25]

The ^{13}C NMR spectrum (at 188 K) of the CD_2Cl_2 mixture obtained by 2 : 1 reaction of $PhOSiMe_3$ with NbF_5 (**3e**) exhibits a pattern including three resonances accounting for *ipso* carbons [δ = 162.6, 162.0, 161.4 ppm], indicating the presence of more than one species. We think that the latter are the trinuclear isomers **3eB** and **3eC**, which differ in the orientation of the phenolato ligands (all equatorial in **3eB**, half equatorial and half axial in **3eC**), see Fig. S11.† This is suggested by the fact that the IR spectrum (solid state) of the mixture matches well the pattern of the superimposed IR spectra computed for **3eB** and **3eC**. The ^{19}F spectrum of **3e** is coherent with the presence of both terminal (120–91 ppm) and bridging (−53 to −65 ppm) fluorines.

The low-temperature NMR spectra of **3a–f** have evidenced, for each case, the formation of a largely prevalent product, bearing symmetrically-distributed alkoxide ligands. Minor isomers have been detected for **3a–d**, while compound **3f** has been obtained as single species.

The DFT study aimed for the identification of the structures adopted by the compounds of general formula $MF_3(OR)_2$ has been extended to **3b**. Hence a group of plausible structures of **3b** have been optimized: they are represented in Fig. S12–S14.†

According to the calculations related to the solvated phase, two trinuclear structures (**3bF**, **3bG**) and two tetranuclear ones (**3bK**, **3bL**) have energies [referred to the $TaF_3(OMe)_2$ unit] whose differences fall within 1 kcal mol^{-1} after addition of the solvation model (Fig. S15†). Conversely dinuclear structures appear not accessible. The trinuclear molecules **3bF** and **3bG** are homologous to **3eB** and **3eC**, respectively, that probably arise in prevalence from NbF_5 + $2PhOSiMe_3$ (see above).

Compounds $TaF_2(OMe)_3$ (4a) and $TaF(OPh)_4$ (5)

The reactions of **1a,b** with three equivalents of $ROSiMe_3$, in CD_2Cl_2 at room temperature, gave complicated mixtures of products.

In the case of $TaF_5/MeOSiMe_3$, the reaction took place clearly with complete consumption of the organic reactant and production of three equivalents of $FSiMe_3$; $TaF_4(OMe)$ and $TaF_3(OMe)_2$ did not form, according to NMR. Therefore the resulting mixture probably corresponded to different forms of $TaF_2(OMe)_3$, **4**.

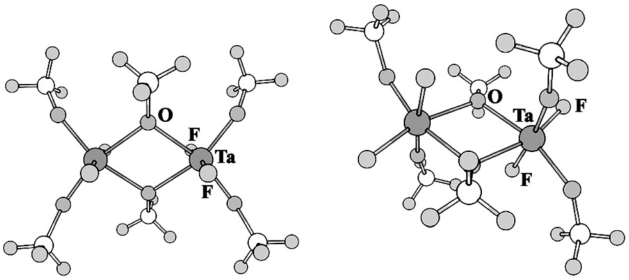

4C **4D**

Fig. 3 Lowest-energy DFT-optimized dinuclear structures of $TaF_2(OMe)_3$ (**4**).

We calculated several possible structures of **4** by a DFT method: the computed structures are shown in Fig. S16–S18 (ESI†), together with the corresponding relative energies. On introduction of the solvation model for CH_2Cl_2, four low-energy structures have energy values [referred to the $TaF_2(OMe)_3$ unit] included in a range of *ca.* 2.5 kcal mol^{-1}. These structures are respectively dinuclear (**4C**, **4D**), trinuclear (**4F**) and tetranuclear (**4H**), see Fig. 3 and Fig. S16–S19 in the ESI.†

The DFT outcome indicates that the dinuclear frame, that appears unfavourable in the cases of $MF_4(OR)$ and $MF_3(OR)_2$ compounds, on theoretical grounds becomes competitive for $TaF_2(OMe)_3$. Interestingly, the ^{19}F NMR spectrum of **4** (in CD_2Cl_2 at 188 K) displays a multitude of resonances due to terminal fluorines (in the range 38–21 and at 16 and 9 ppm), and only very low-intensity signals at negative values of chemical shifts (δ = −101, −104, −110 ppm), see Experimental. This fact suggests that dinuclear species lacking bridging fluorines (presumably **4C** and **4D**) largely prevail in the mixture.[26] The preference of alkoxide ligands for bridging positions is a typical feature of dinuclear Nb(V) and Ta(V) halide-alkoxides.[6b,c,f]

In a number of cases, NMR analyses (see the Experimental section, NMR studies) on the mixtures obtained by the reaction of MF_5 with 3 equiv. of $ROSiMe_3$ pointed out the presence of variable amounts of unreacted organic material, and/or the production of some $MF_3(OR)_2$ (**2**). This evidence implies that the clean synthesis of $MF_2(OR)_3$ compounds is not generally viable with the present method, at least at room temperature. In other words, the stepwise substitution of [F] ligands by [OR] groups in dichloromethane, starting from MF_5, seems to become increasingly less favourable on decreasing the fluorine content. This trend has been detailed for M = Ta and R = Me, see eqn (3)–(5) (referring to the most stable structures).

$$TaF_5 + MeOSiMe_3 \rightarrow TaF_4(OMe) + FSiMe_3 \quad \Delta H_{calc} = -61\ \text{kcal mol}^{-1} \tag{3}$$

$$TaF_4(OMe) + MeOSiMe_3 \rightarrow TaF_3(OMe)_2 + FSiMe_3 \quad \Delta H_{calc} = -30\ \text{kcal mol}^{-1} \tag{4}$$

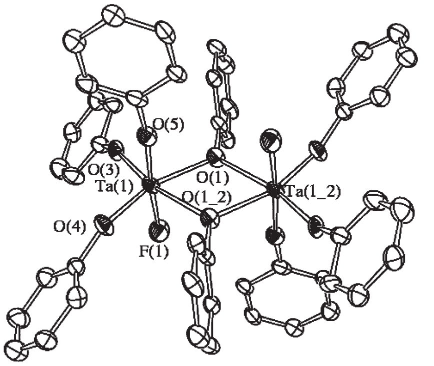

Fig. 4 Molecular structure of [TaF(OPh)$_3$(μ-OPh)]$_2$, **5A**, with key atoms labelled. The H-atoms have been omitted for clarity. Thermal ellipsoids are at the 50% probability level.

Table 2 Selected bond distances (Å) and angles (°) for **5A**[a]

Ta(1)–F(1)	1.901(6)	Ta(1)–O(5)	1.891(7)
Ta(1)–O(3)	1.875(6)	Ta(1)–O(4)	1.879(7)
Ta(1)–O(1)	2.113(7)	Ta(1)–O(1_2)	2.100(6)
Ta(1)–O(1)–Ta(1_2)	111.2(3)	O(1)–Ta(1)–O(1_2)	68.8(3)

[a] Symmetry transformations used to generate equivalent atoms: $-x$, $-y-1$, $-z$.

$$\mathrm{TaF_3(OMe)_2 + MeOSiMe_3 \rightarrow TaF_2(OMe)_3 + FSiMe_3} \quad \Delta H_{\mathrm{calc}} = -23\ \mathrm{kcal\ mol^{-1}} \tag{5}$$

On an average, a maximum of three equivalents of fluoride ligands in MF$_5$ undergo substitution with –OR groups by reaction with ROSiMe$_3$, in CD$_2$Cl$_2$ at room temperature. According to NMR analyses, the 1 : 4 and 1 : 5 reactions produced only three equivalents of FSiMe$_3$ per mole of the metal (see the Experimental section, NMR studies).

In spite of this fact, crystals of the tetrasubstituted product [TaF(OPh)$_3$(μ-OPh)]$_2$ (**5A**) could be collected from a CH$_2$Cl$_2$ mixture obtained by a prolonged reaction of TaF$_5$ with a large excess of PhOSiMe$_3$. X-ray analysis was carried out on **5A**: the ORTEP representation is shown in Fig. 4, whereas relevant bond lengths and angles are reported in Table 2. The unit cell contains discrete dinuclear [TaF(OPh)$_3$(μ-OPh)]$_2$ molecules, which reside on a crystallographic inversion centre. The dinuclear species adopts an edge sharing bioctahedral geometry, with one terminal F-ligand (in the axial position), three terminal and two bridging OPh ligands. The two F-ligands on the different Ta-atoms are in relative *trans* position with respect to the equatorial plane comprising the Ta-atoms and the two bridging phenoxides. The Ta–O and O–C distances are comparable with those previously reported for Ta(v) aryloxides.[5g,h,27] In particular, the bridging OPh ligand is almost symmetric [O(1)–Ta(1) 2.113(7) Å; O(1_2)–Ta(1) 2.100(6) Å]. The Ta–O$_{\mathrm{bridging}}$ contacts are considerably elongated compared to the Ta–O$_{\mathrm{terminal}}$ ones [average: 1.882(12) Å], in analogy with what was reported for [Ta(OTol)$_3$-(μ-OTol)]$_2$ (Tol = 4-C$_6$H$_4$Me).[5h]

Different, possible isomers of [TaF(OPh)$_4$]$_2$ were the object of DFT investigation: the respective computed molecular structures (**5A–C**) are represented in Fig. S20.†

The structures **5A** and **5B** bear two bridging phenoxides and differ by the orientation of the F-ligands (*i.e. axial* in **5A**, *equatorial* in **5B**). They present very close energies in CH$_2$Cl$_2$ ($\Delta E_{\mathrm{calc}} \approx 0.1$ kcal mol^{-1}). Conversely structure **5C**, bearing two bridging fluorides, is less stable than both **5A** and **5B** by *ca.* 6 kcal mol^{-1}. A list of the main calculated geometric parameters of **5A** is provided in Table S2,† showing a good agreement with the X-ray data.

We tried to force the selective formation of **5** by high temperature reaction of TaF$_5$ with PhOSiMe$_3$, in a 4 : 1 ratio. The reaction was carried out in CDCl$_3$ in a sealed tube at *ca.* 90 °C for several hours, and afforded a yellow mixture which was analyzed by NMR. The NMR data indicate the formation of four equivalents of FSiMe$_3$ and different metal species (see Experimental). The ^{19}F pattern may be attributed to the presence in solution of **5A** and **5B**, and of a third product containing bridging fluorines. The latter is likely not to coincide with **5C** (see above), and may hold nuclearity higher than two.

Conclusions

A series of polynuclear fluoride-alkoxides of niobium and tantalum in the highest oxidation state, MF$_x$(OR)$_{5-x}$ (x = 2–4), have been prepared and spectroscopically characterized. The reactions of MF$_5$ with different amounts of trimethylsilyl ethers, in a chlorinated solvent, take place to afford metal products of given empirical formulas. However mixtures of isomers and/or species with different nuclearity may form in some cases. Although DFT calculations have been not really conclusive in the determination of the nuclearities of the new compounds, the formation of tetra- and trinuclear products appears favourable for both MF$_4$(OMe) and MF$_3$(OMe)$_2$. Dinuclear frames become energetically competitive on further decreasing the fluorine content.

Spectroscopic data and DFT outcomes agree in that highly-symmetric molecules are produced prevalently, and the –OR ligands preferentially occupy terminal sites in MF$_4$(OR) and MF$_3$(OR)$_2$, but bridging sites in TaF$_2$(OMe)$_3$ and TaF(OPh)$_4$.

The X-ray structures of [NbF$_2$(μ-F)(OPh)$_2$]$_3$ and [TaF(OPh)$_3$-(μ-OPh)]$_2$, which represent the first examples of crystallographic characterizations of niobium/tantalum fluoride-alkoxides(aryloxides), show agreement with both the spectroscopic features and the computer results.

Experimental

General

All the metal compounds cited herein are air/moisture sensitive and were manipulated under an atmosphere of pre-purified argon using standard Schlenk techniques. The reaction vessels were oven dried at 140 °C prior to use, evacuated (10^{-2} mm Hg) and then filled with argon. NbF$_5$, **1a**, and TaF$_5$, **1b**, were purchased from Strem (99.5% purity), stored as received in sealed tubes under argon, and used without further purification. Solvents (Sigma-Aldrich) were distilled from P$_4$O$_{10}$ before use. ROSiMe$_3$ (R = Me, Et, Ph; Sigma-Aldrich) and CD$_2$Cl$_2$ (Cortecnet) were stored under an argon atmosphere as received. Infrared spectra were recorded at 298 K on a FT IR-Perkin Elmer

Spectrometer, equipped with a UATR sampling accessory. ^{1}H, ^{13}C and ^{19}F NMR spectra were recorded on a Varian Gemini 200BB instrument; ^{93}Nb NMR spectra were recorded on a Bruker Avance DRX400 instrument equipped with a BBFO broadband probe. The chemical shifts for ^{1}H and ^{13}C were referenced to the non-deuterated aliquot of the solvent; the chemical shifts for ^{19}F were referenced to external $CFCl_3$; the chemical shifts for ^{93}Nb were referenced to external $[NEt_4][NbCl_6]$.

Conductivity measurements were carried out on CH_2Cl_2 solutions with an Eutech Con 700 Instrument (cell constant = 1.0 cm^{-1}).[28] Carbon and hydrogen analyses were performed on a Carlo Erba mod. 1106 instrument. The fluoride content was determined by a fluoride ion selective electrode, after boiling the sample in an alkaline solution. The metal was analyzed as M_2O_5 obtained by high temperature treatment of the solid sample with a HNO_3 solution, followed by calcination in a platinum crucible. The metal analyses were repeated twice in order to check for reproducibility.

Synthesis isolation and characterization of $MF_4(OR)$, $MF_3(OR)_2$ and $MF_2(OR)_3$

General procedure: $ROSiMe_3$ was added to a suspension of MF_5 (0.80 mmol) in CH_2Cl_2 (10 mL), in the appropriate molar ratio, and the mixture was stirred at room temperature for 5–10 h. Progressive dissolution of the solid was observed. The volatile materials were removed *in vacuo*; the product was isolated in the solid state by the treatment of the residue with $CHCl_3$ (2 mL) and pentane (15 mL). NMR analyses were carried out on CD_2Cl_2 solutions (*ca.* 0.7 mL) prepared by addition of the appropriate amount of $ROSiMe_3$ to MF_5.

$NbF_4(OMe)$, 2a. White solid, yield 80%. Anal. calcd for CH_3F_4NbO: C, 6.01; H, 1.51; Nb, 46.47; F, 38.01. Found: C, 6.18; H, 1.32; Nb, 45.80; F, 37.82. IR (solid state): 2946w, 1444w, 1393w, 1112s (ν_{CO}), 983m, 737vs cm^{-1}. ^{1}H NMR (CD_2Cl_2, 298 K): δ = 4.60 (s, Me) ppm. ^{13}C NMR{^{1}H} (CD_2Cl_2, 298 K): δ = 76.6 (Me) ppm. ^{1}H NMR (CD_2Cl_2, 188 K): δ = 4.69, 4.59, 4.49, 3.93, 3.84 (s, Me, ratio 8 : 6 : 4 : 1 : 2) ppm. ^{13}C NMR{^{1}H} (CD_2Cl_2, 188 K): δ = 75.9–73.5 (Me) ppm. ^{19}F NMR (CD_2Cl_2, 188 K): δ = 177–161, 148–127, 96–85 (m, 3 F, $F_{terminal}$), −60 (m, 1 F, $F_{bridging}$) ppm. ^{93}Nb NMR (CD_2Cl_2, 223 K): δ = 1050 ($\Delta\nu^{1}/_{2}$ = 8 × 10^{4} Hz) ppm.

$TaF_4(OMe)$, 2b. Colourless solid, yield 76%. Anal. calcd for CH_3F_4OTa: C, 4.17; H, 1.05; Ta, 62.83; F, 26.39. Found: C, 4.32; H, 0.97; Ta, 61.68; F, 26.60. IR (solid state): 2957w, 1448w, 1395w, 1138vs (ν_{CO}), 972m, 871m, 826m, 679m cm^{-1}. ^{1}H NMR (CD_2Cl_2, 188 K): δ = 4.79, 4.04, 3.94 (s, Me, ratio 20 : 1 : 1.5) ppm. ^{19}F NMR (CD_2Cl_2, 188 K): δ = 120–93, 76–65, 32 (m, 4 F, $F_{terminal}$), −82.0 (s-br, 1 F, $F_{bridging}$) ppm.

$NbF_4(OEt)$, 2c. Colourless rubbery solid, yield 77%. Anal. calcd for $C_2H_5F_4NbO$: C, 11.23; H, 2.36; Nb, 43.42; F, 35.52. Found: C, 11.03; H, 2.54; Nb, 42.85; F, 35.79. IR (solid state): 2992w, 2942w, 1467w, 1385w, 1096s and 1063vs (ν_{CO}), 944m, 901m, 864m, 804m cm^{-1}. ^{1}H NMR (CD_2Cl_2, 298 K): δ = 4.96 (br, 2 H, CH_2), 1.57 (br, 3 H, CH_3) ppm. ^{1}H NMR (CD_2Cl_2, 183 K): δ = 4.90 (br, 2 H, CH_2), 1.45 (br, 3 H, CH_3) ppm. ^{13}C NMR{^{1}H} (CD_2Cl_2, 188 K): δ = 85.5 (major, CH_2), 84.5 (minor, CH_2), 16.5 (CH_3) ppm. ^{19}F NMR (CD_2Cl_2, 188 K): δ = 172–162, 146–128, 94–85 (m, 3 F, $F_{terminal}$), −50 to −62 (s-br, 1 F, $F_{bridging}$) ppm. Λ_M (293 K) = 0.2 S cm^{2} mol^{-1}.

$TaF_4(OEt)$, 2d. Colourless rubbery solid, yield 75%. Anal. calcd for $C_2H_5F_4OTa$: C, 7.95; H, 1.67; Ta, 59.92; F, 25.16. Found: C, 8.28; H, 1.55; Ta, 60.12; F, 25.42. IR (solid state): 2991w, 1450w, 1389w, 1270w, 1110vs and 1084s (ν_{CO}), 1007w-m, 946w-m, 896m, 853m cm^{-1}. ^{1}H NMR (CD_2Cl_2, 183 K): δ = 5.22, 4.73 (q, $^{3}J_{HH}$ = 7 Hz, 2 H, CH_2, ratio 20 : 1), 1.60 (t, $^{3}J_{HH}$ = 7 Hz, 3 H, CH_3) ppm. ^{13}C NMR{^{1}H} (CD_2Cl_2, 188 K): δ = 81.6 (CH_2), 16.7 (CH_3) ppm. ^{19}F NMR (CD_2Cl_2, 188 K): δ = 153–141, 115–99, 76–66 (m, 2.8 F, $F_{terminal}$), −67, −81 (s-br, 1 F, $F_{bridging}$) ppm.

$NbF_4(OPh)$, 2e. Yellow solid, yield 84%. Anal. calcd for $C_6H_5F_4NbO$: C, 27.51; H, 1.92; Nb, 35.46; F, 29.00. Found: C, 27.33; H, 1.80; Nb, 35.21; F, 28.75. IR (solid state): 1587m, 1479m-s, 1224m, 1162m and 1069w (ν_{CO}), 1021w, 898vs, 750vs, 684vs cm^{-1}. ^{1}H NMR (CD_2Cl_2, 298 K): δ = 7.38–7.17 (Ph) ppm. ^{13}C NMR{^{1}H} (CD_2Cl_2, 298 K): δ = 162.5 (*ipso*-Ph), 129.9, 128.0, 119.4 (Ph) ppm. ^{1}H NMR (CD_2Cl_2, 188 K): δ = 7.42–6.93 (Ph) ppm. ^{13}C NMR{^{1}H} (CD_2Cl_2, 188 K): δ = 162.7 (*ipso*-Ph), 130.2, 128.8, 120.1 (Ph) ppm. ^{19}F NMR (CD_2Cl_2, 188 K): δ = 198–189, 156–140 (m, 2.2 F, $F_{terminal}$), −48 to −64 (m, 1 F, $F_{bridging}$) ppm. ^{93}Nb NMR (CD_2Cl_2, 223 K): δ = 1083 ($\Delta\nu^{1}/_{2}$ = 4 × 10^{4} Hz) ppm.

$TaF_4(OPh)$, 2f. Pale yellow solid, yield 85%. Anal. calcd for $C_6H_5F_4OTa$: C, 20.59; H, 1.44; Ta, 51.69; F, 21.71. Found: C, 20.86; H, 1.29; Ta, 51.35; F, 21.84. IR (solid state): 3069w, 1587m, 1480s, 1455w, 1249s-sh, 1223s, 1163m (ν_{CO}), 1069w, 1023w, 1001w, 916m, 842m, 750vs, 684s cm^{-1}. ^{1}H NMR (CD_2Cl_2, 188 K): δ = 7.40–7.05 (Ph) ppm. ^{13}C NMR {^{1}H} (CD_2Cl_2, 188 K): δ = 159.7 (*ipso*-Ph), 129.9, 127.7, 119.8 (Ph) ppm. ^{19}F NMR (CD_2Cl_2, 188 K): δ = 156–149, 128–107, 88–85 (m, 2.6 F, $F_{terminal}$), −66 to −84 (m, 1 F, $F_{bridging}$) ppm.

$NbF_3(OMe)_2$, 3a. Very light blue solid, yield 73%. Anal. calcd for $C_2H_6F_3NbO_2$: C, 11.33; H, 2.85; Nb, 43.83; F, 26.89. Found: C, 11.20; H, 3.01; Nb, 43.42; F, 26.60. IR (solid state): 2939w, 2839w, 1447w, 1260w, 1117s-sh and 1070vs (ν_{CO}), 992m, 852w-m, 798m cm^{-1}. ^{1}H NMR (CD_2Cl_2, 298 K): δ = 4.49 (s, Me) ppm. ^{13}C NMR{^{1}H} (CD_2Cl_2, 298 K): δ = 68.4 (Me) ppm. ^{1}H NMR (CD_2Cl_2, 223 K): δ = 4.50, 4.40, 3.89 (s, Me, ratio 6 : 1 : 0.2) ppm. ^{13}C NMR{^{1}H} (CD_2Cl_2, 223 K): δ = 68.9 (br, Me) ppm. ^{19}F NMR (CD_2Cl_2, 211 K): δ = 114–106, 93, 88–80, 73–68 (m, 1.5 F, $F_{terminal}$), −71.0 to −77.3 (m, 1 F, $F_{bridging}$) ppm. ^{93}Nb NMR (CD_2Cl_2, 223 K): δ = 1080 ($\Delta\nu^{1}/_{2}$ = 2.5 × 10^{4} Hz) ppm.

$TaF_3(OMe)_2$, 3b. Colourless rubbery solid, yield 78%. Anal. calcd for $C_2H_6F_3O_2Ta$: C, 8.01; H, 2.02; Ta, 60.31; F, 19.00. Found: C, 7.83; H, 2.11; Ta, 60.13; F, 19.10. IR (solid state): 2990w, 1386w, 1111s (ν_{CO}), 986m, 879s, 735s cm^{-1}. ^{1}H NMR

(CD_2Cl_2, 188 K): δ = 4.50, 4.40 (s, Me, ratio 13 : 4) ppm. ^{13}C NMR{^1H} (CD_2Cl_2, 188 K): δ = 66.8–66.4 (br, Me) ppm.

$NbF_3(OEt)_2$, 3c. Colourless viscous liquid, yield 74%. Anal. calcd for $C_4H_{10}F_3NbO_2$: C, 20.02; H, 4.20; Nb, 38.71; F, 23.75. Found: C, 19.96; H, 4.14; Nb, 38.12; F, 23.94. ^1H NMR (CD_2Cl_2, 188 K): δ = 4.63 (br, 2 H, CH_2), 1.34 (br, 3 H, CH_3) ppm. ^{13}C NMR{^1H} (CD_2Cl_2, 188 K): δ = 78.6 (minor, CH_2), 78.0 (major, CH_2), 17.2 (CH_3) ppm. ^{19}F NMR (CD_2Cl_2, 188 K): δ = 102–77 (m, 1.8 F, $F_{terminal}$), −69 to −76 (m, 1 F, $F_{bridging}$) ppm.

$TaF_3(OEt)_2$, 3d. Colourless viscous liquid, yield 73%. Anal. calcd for $C_4H_{10}F_3O_2Ta$: C, 14.64; H, 3.07; Ta, 55.16; F, 17.37. Found: C, 14.32; H, 3.19; Ta, 54.86; F, 17.12. ^1H NMR (CD_2Cl_2, 183 K): δ = 4.93 (br, 2 H, CH_2), 1.34 (br, 3 H, CH_3) ppm. ^{13}C NMR{^1H} (CD_2Cl_2, 188 K): δ = 80.2 (major, CH_2), 79.2 (minor, CH_2), 16.8 (CH_3) ppm. ^{19}F NMR (CD_2Cl_2, 188 K): δ = 106–92, 72–63, 38–30 (m, 3.3 F, $F_{terminal}$), −80 to −86 (m, 1 F, $F_{bridging}$) ppm.

$NbF_3(OPh)_2$, 3e. Yellow powder, yield 86%. Anal. calcd for $C_{12}H_{10}F_3NbO_2$: C, 42.88; H, 3.00; Nb, 27.64; F, 16.96. Found: C, 42.53; H, 3.11; Nb, 27.21; F, 16.49. IR (solid state): 1633w, 1587m, 1479vs, 1231vs, 1162m (ν_{CO}), 1069w-m, 863vs, 804vs, 749vs cm^{-1}. ^1H NMR (CD_2Cl_2, 298 K): δ = 7.19, 7.08 (Ph) ppm. ^{13}C NMR{^1H} (CD_2Cl_2, 298 K): δ = 162.7 (*ipso*-Ph), 129.8, 125.9, 119.3 (Ph) ppm. ^1H NMR (CD_2Cl_2, 211 K): δ = 7.36–6.95 (Ph) ppm. ^{13}C NMR{^1H} (CD_2Cl_2, 188 K): δ = 162.6, 161.4 (minor, *ipso*-Ph), 162.0 (major, *ipso*-Ph), 129.4, 126.1, 125.1, 120.5, 119.2 (Ph) ppm. ^{19}F NMR (CD_2Cl_2, 188 K): δ = 120–91 (m, 1.5 F, $F_{terminal}$), −53 to −65 (m, 1 F, $F_{bridging}$) ppm. ^{93}Nb NMR (CD_2Cl_2, 223 K): δ = 1172 ($\Delta\nu^1/_2$ = 2.4 × 10^3 Hz) ppm. Few crystals of $[NbF_2(\mu\text{-}F)(OPh)_2]_3$ (**3eB**) suitable for X-ray analysis were collected from a CH_2Cl_2 solution layered with pentane and stored at −30 °C for a few days.

$TaF_3(OPh)_2$, 3f. Yellow powder, yield 81%. Anal. calcd for $C_{12}H_{10}F_3O_2Ta$: C, 33.98; H, 2.38; Ta, 42.66; F, 13.44. Found: C, 34.21; H, 2.44; Ta, 41.76; F, 13.28. ^1H NMR (CD_2Cl_2, 188 K): δ = 7.40–7.00 (Ph) ppm. ^{13}C NMR{^1H} (CD_2Cl_2, 188 K): δ = 158.1 (*ipso*-Ph), 128.2, 123.4, 122.1, 117.6 (Ph) ppm. ^{19}F NMR (CD_2Cl_2, 188 K): δ = 66–58, 38–22 (m, $F_{terminal}$), −86 to −105 (m-br, $F_{bridging}$) ppm.

$TaF_2(OMe)_3$, 4. Colourless solid, yield 79%. Anal. calcd for $C_3H_9F_2O_3Ta$: C, 11.55; H, 2.91; Ta, 57.99; F, 12.18. Found: C, 11.84; H, 3.06; Ta, 57.53; F, 12.37. ^1H NMR (CD_2Cl_2, 188 K): δ = 4.47, 4.40, 4.31, 4.22, 4.17, 4.12 (s, Me, ratio 4 : 5 : 4 : 1 : 1.2 : 1) ppm. ^{13}C NMR{^1H} (CD_2Cl_2, 188 K): δ = 64.3 (major), 63.8, 63.3, 62.4, 62.0, 61.1 (br, Me) ppm. ^{19}F NMR (CD_2Cl_2, 188 K): δ = 38–21, 16, 9 (m, 27 F, $F_{terminal}$), −101, −104, −110 (m, 1 F, $F_{bridging}$) ppm.

Synthesis and isolation of $TaF(OPh)_4$, 5

TaF_5 (0.250 mmol), $CDCl_3$ (0.60 mL), 1,2-dichloroethane (0.250 mmol) and $PhOSiMe_3$ (1.00 mmol) were introduced into a NMR tube in the order given. The tube was sealed, then the mixture was heated at *ca.* 90 °C for 12 h. A yellow mixture was obtained. NMR analyses showed the absence of $PhOSiMe_3$ and the formation of $FSiMe_3$ ($FSiMe_3$: 1,2-dichloroethane ≈ 4). Resonances related to metal products appeared as follows. ^1H NMR ($CDCl_3$, 213 K): δ = 7.40–6.11 (Ph). ^{13}C NMR{^1H} ($CDCl_3$, 213 K): δ = 161.4, 161.0 (major, *ipso*-Ph), 160.3, 159.4, 159.0 (minor, *ipso*-Ph); 129.5, 129.1, 128.8, 124.5, 123.2, 122.6, 121.7, 121.4, 120.1, 119.2 ppm. ^{19}F NMR ($CDCl_3$, 213 K): δ = 47.8 (s, 0.1 F), 35.7 (s, 0.2 F), 33.4 (s, 1.1 F), 32.5 (s, 1.5 F), −89.8 (s, 1.0 F), −91.3 (s, 0.1 F) ppm. IR and elemental analyses were carried out on the yellow powder obtained upon removal of the volatile materials. Anal. calcd for $C_{12}H_{10}F_3O_2Ta$: C, 50.36; H, 3.52; Ta, 31.61; F, 13.44. Found: C, 50.16; H, 3.39; Ta, 31.15; F, 13.22. IR (solid state): 3063w, 1586m, 1477vs, 1452w-m, 1284m, 1226vs, 1182s, 1161s, 1067m, 1022m, 1000w-m, 891vs, 861m, 811s, 765m, 747vs, 684s cm^{-1}. Few crystals of $[TaF(OPh)_3(\mu\text{-}OPh)]_2$ (**5A**) suitable for X-ray analysis were collected from a CH_2Cl_2 mixture obtained by treatment of TaF_5 (*ca.* 1.2 mmol) with excess $PhOSiMe_3$ (reaction time = 72 h), layered with pentane and stored at −30 °C for one week.

NMR studies

The reactions of MF_5 (0.40–0.80 mmol) with 1–5 equiv. of $ROSiMe_3$ were performed in CD_2Cl_2 solutions in sealed NMR tubes in the presence of $CHCl_3$ as standard ($CHCl_3$/M ratio = 1). ^1H, ^{13}C and ^{19}F NMR spectra were recorded after 48 h. Complete consumption of $ROSiMe_3$ was observed in the reactions of MF_5 with 1–3 equiv. of $ROSiMe_3$. Unreacted $ROSiMe_3$ was found in the mixtures obtained from MF_5 and 4–5 equiv. of $ROSiMe_3$. $MeOSiMe_3$: δ(^1H, $CDCl_3$) = 3.44 (s, 3 H, OMe), 0.13 (s, 9 H, $SiMe_3$) ppm. $EtOSiMe_3$: δ(^1H, $CDCl_3$) = 3.67 (q, 2 H, $^3J_{HH}$ = 7.33 Hz, CH_2), 1.21 (t, 3 H, $^3J_{HH}$ = 7.33 Hz, CH_2CH_3), 0.13 (s, 9 H, $SiMe_3$) ppm. $PhOSiMe_3$: δ(^1H, $CDCl_3$) = 7.31–6.86 (m, 5 H, Ph), 0.30 (s, 9 H, $SiMe_3$) ppm; δ(^{13}C, $CDCl_3$) = 155.3 (*ipso*-Ph), 129.5, 121.5, 120.1 (Ph), 0.23 ($SiMe_3$) ppm. Some unreacted $ROSiMe_3$ (*ca.* 0.4 equiv.) was detected from NbF_5 + 3 $PhOSiMe_3$ and TaF_5 + 3 $EtOSiMe_3$, respectively. $FSiMe_3$ was detected in the final mixtures [δ(^1H, CD_2Cl_2) = 0.25 ppm, $^3J_{HF}$ = 7.33 Hz; δ(^{13}C, CD_2Cl_2) = 0.34 ppm, $^2J_{CF}$ = 14.5 Hz; δ(^{19}F, CD_2Cl_2) = −158.3 ppm] in variable amounts: $FSiMe_3/CHCl_3$ = 1 from MF_5 + 1 $ROSiMe_3$; $FSiMe_3/CHCl_3$ = 2 from MF_5 + 2 $Si(OR)Me_3$; $FSiMe_3/CHCl_3$ ≈ 3 from MF_5 + 3 $ROSiMe_3$; $FSiMe_3/CHCl_3$ ≈ 3 from MF_5 + 4 $ROSiMe_3$; $FSiMe_3/CHCl_3$ ≈ 3 from MF_5 + 5 $ROSiMe_3$.

X-ray crystallographic study

Crystal data and collection details for $[NbF_2(\mu\text{-}F)(OPh)_2]_3\cdot 0.5C_6H_{14}$ (**3eB·C_6H_{14}**) and $[TaF(OPh)_3(\mu\text{-}OPh)]_2$ (**5A**) are reported in Table 3. The diffraction experiments were carried out on a Bruker Apex II diffractometer equipped with a CCD detector using Mo-Kα radiation. Data were corrected for Lorentz polarization and absorption effects (empirical absorption correction SADABS).[29] Structures were solved by direct methods and refined by full-matrix least-squares based on all data using F^2.[30] All non-hydrogen atoms were refined with anisotropic displacement parameters, apart from the C_6H_{14} molecule in **3eB·C_6H_{14}** which was treated isotropically. H-atoms were placed in

Table 3 Crystal data and experimental details for $[NbF_2(\mu\text{-}F)(OPh)_2]_3\cdot C_6H_{14}$ (**3eB·C_6H_{14}**) and $[TaF(OPh)_3(\mu\text{-}OPh)]_2$ (**5A**)

Complex	**3eB**·C_6H_{14}	**5A**
Formula	$C_{39}H_{37}F_9Nb_3O_6$	$C_{48}H_{40}F_2O_8Ta_2$
F_w	1051.42	1144.70
T (K)	100(2)	100(2)
λ (Å)	0.71073	0.71073
Crystal system	Triclinic	Triclinic
Space group	$P\bar{1}$	$P\bar{1}$
a (Å)	9.5980(18)	9.940(4)
b (Å)	11.661(2)	10.003(4)
c (Å)	18.367(3)	12.384(5)
α (°)	83.930(2)	68.033(4)
β (°)	75.313(2)	86.135(4))
γ (°)	86.150(2)	68.477(4)
Cell volume (Å^3)	1975.6(6)	1058.8(7)
Z	2	1
D_c (g cm^{-3})	1.768	1.795
μ (mm^{-1})	0.944	5.227
F(000)	1046	556
Crystal size (mm)	0.18 × 0.15 × 0.11	0.16 × 0.14 × 0.11
θ limits (°)	1.76–25.03	1.78–25.03
Reflections collected	18 800	9079
Independent reflections	6969 [R_{int} = 0.1081]	3583 [R_{int} = 0.0573]
Data/restraints/parameters	6969/492/573	3583/144/271
Goodness of fit on F^2	0.977	1.011
R_1 ($I > 2\sigma(I)$)	0.0585	0.0536
wR_2 (all data)	0.1550	0.1354
Largest diff. peak/hole (e Å^{-3})	0.895/−0.885	5.382/−1.616

calculated positions and treated isotropically using the 1.2 fold U_{iso} value of the parent atom except for methyl protons, which were assigned the 1.5 fold U_{iso} value of the parent C-atom. Similar U restraints were applied to C-atoms (s.u. 0.01). Two phenyl rings in **3eB·C_6H_{14}** are disordered. Disordered atomic positions were split and refined using one occupancy parameter per disordered group. The C_6H_{14} molecule in **3eB·C_6H_{14}** is disordered over two positions related by an inversion centre: the independent image has been, therefore, refined with a 0.5 occupancy factor and restraining the C–C bond distances (s.u. 0.01) to 1.47 Å. Large residual electron density is present in **5A** close to the tantalum atoms, due to the strong absorption of the heavy atoms.

CCDC reference numbers 876459 (**3eB**) and 876460 (**5A**) contain the supplementary crystallographic data for this paper.

Computational studies

The computational geometry optimisation of the complexes was carried out using the hybrid DFT M06 functional[31] without symmetry constraints, in combination with a polarized triple-ζ quality basis set composed of the 6-311G(d,p) basis set on the light atoms and the LANL2TZ(f) basis set on the metal centres.[32] Implicit solvation was added by using the C-PCM model for dichloromethane.[33] The "restricted" formalism was applied in all the calculations. The stationary points were characterized as true minima by IR simulations, from which zero-point vibrational energies were obtained.[25] The software used was Gaussian 09.[34] The simulations were performed at CINECA (Centro Italiano di Supercalcolo, Bologna, Italy) using a IBM P6-575 workstation equipped with 64-bit IBM Power6 processors.

Acknowledgements

The authors thank the Ministero dell'Istruzione, dell'Università e della Ricerca (PRIN 2009 project: 'New strategies for the control of reactions: interactions of molecular fragments with metallic sites in unconventional species') for financial support and the CINECA Award N. HP10CRPVUO 2011 for the availability of high performance computing resources and support.

Notes and references

1 (*a*) F. Marchetti and G. Pampaloni, *Chem. Commun.*, 2012, **48**, 635 and references therein; (*b*) G. Pampaloni and A. M. Raspolli Galletti, *Coord. Chem. Rev.*, 2010, **254**, 525; (*c*) M. O. Guerrero-Pérez and M. A. Bañares, *Catal. Today*, 2009, **142**, 245; (*d*) R. Arteaga-Müller, H. Tsurugi, T. Saito, M. Yanagawa, S. Oda and K. Mashima, *J. Am. Chem. Soc.*, 2009, **131**, 5370; (*e*) A. Spannenberg, H. Fuhrmann, P. Arndt, W. Baumann and R. Kempe, *Angew. Chem., Int. Ed.*, 1998, **37**, 3363.

2 (*a*) F. Marchetti, G. Pampaloni, Y. Patil, A. M. Raspolli Galletti and S. Zacchini, *J. Polym. Sci., Part A: Polym. Chem.*, 2011, **49**, 1664; (*b*) A. Kanazawa, S. Kanaoka and S. Aoshima, *J. Polym. Sci., Part A: Polym. Chem.*, 2010, **48**, 2509; (*c*) T. B. Do, M. Cai and M. S. Ruthkosky, *Patent WO 2009/152003 A2*, GM Global Technology Operations), Inc., 2009; (*d*) R. Petroff Saint-Arroman, B. Didillon, A. de Mallmann, J. M. Basset and F. Lefebvre, *Appl. Catal., A*, 2008, **337**, 78; (*e*) J. Choi, J. Kang, J. Song, B. Park, C. Kang and S. Noh, *Patent WO 2008/039015 A1*, LG Chem, LTD. and LG Petrochemical Co., LTD., 2008; (*f*) A. Di Benedetto and M. Aresta, *Catal. Today*, 2006, **115**, 88.

3 (*a*) L. Appel, R. Fiz, W. Tyrra and S. Mathur, *Dalton Trans.*, 2012, **41**, 1981; (*b*) Y. Nakashima, W. Sakamoto and T. Yogo, *J. Eur. Ceram. Soc.*, 2011, **31**, 2497; (*c*) A. Chowdhury, J. Bould, M. G. S. Londesborough and S. J. Milne, *J. Solid State Chem.*, 2011, **184**, 317; (*d*) S. Mishra, E. Jeanneau, M.-H. Berger, J.-F. Hochepied and S. Daniele, *Inorg. Chem.*, 2010, **49**, 11184; (*e*) V. Boffa, H. L. Castricum, R. Garcia, R. Schmuhl, A. V. Petukhov, D. H. A. Blank and J. E. ten Elshof, *Chem. Mater.*, 2009, **21**, 1822; (*f*) G. A. Seisenbaeva, V. G. Kessler, R. Pazik and W. Strek, *Dalton Trans.*, 2008, 3412; (*g*) Z. Xu, S. Wang, J. Ren, Y. Liu and Z. Fang, *Dyes Pigm.*, 2008, **79**, 140; (*h*) E. Rauwel, G. Clavel, M.-G. Willinger, P. Rauwel and N. Pinna, *Angew. Chem., Int. Ed.*, 2008, **47**, 3592; (*i*) G. H. Thomas, E. D. Specht, J. Z. Larese, Z. B. Xue and D. B. Beach, *J. Mater. Res.*, 2008, **23**, 3281; (*j*) U. Schubert, *Acc. Chem. Res.*, 2007, **40**, 730.

4 Some recent references are: (*a*) B. Knabe, D. Schütze, T. Jungk, M. Svete, W. Assenmacher, W. Mader and K. Buse, *Phys. Status Solidi A*, 2011, **208**, 857; (*b*) Y. Suyama, T. Yamada, Y. Hirano, K. Takamura and K. Takahashi, *Adv. Sci. Technol.*, 2010, **63**, 7; (*c*) S. Furiukawa, H. Amino, S. Iwamoto and M. Inoue, *J. Phys.: Conf. Ser.*, 2008, **121**, 082006; (*d*) Z. Cheng, K. Ozawa, M. Osada, A. Miyazaki and A. Kimura, *J. Am. Ceram. Soc.*, 2006, **89**, 1188.

5 (*a*) G. G. Nunes, G. A. Seisenbaeva and V. G. Kessler, *J. Sol-Gel Sci. Technol.*, 2007, **43**, 105; (*b*) R. N. Kapoor, F. Cervantes-Lee, C. F. Campana, C. Haltiwanger, K. Abney and K. H. Pannell, *Inorg. Chem.*, 2006, **45**, 2203; (*c*) T. J. Boyle, J. J. Gallegos III, D. M. Pedrotty, E. R. Mechenbier and B. L. Scott, *J. Coord. Chem.*, 1999, **47**, 155; (*d*) S. C. Goel, J. A. Hollingsworth, A. M. Beatty, K. D. Robinson and W. E. Buhro, *Polyhedron*, 1998, **17**, 781; (*e*) T. J. Boyle, T. M. Alam, D. Dimos, G. J. Moore, C. D. Buchheit, H. N. Al-shareef, E. R. Mechenbier and B. R. Bear, *Chem. Mater.*, 1997, **9**, 3187; (*f*) T. W. Coffindaffer, B. D. Steffy, I. P. Rothwell, K. Folting, J. C. Huffman and W. E. Streib, *J. Am. Chem. Soc.*, 1989, **111**, 4742; (*g*) R. Wang, K. Folting, J. C. Huffman, L. R. Chamberlain and I. P. Rothwell, *Inorg. Chim. Acta*, 1986, **120**, 81; (*h*) L. N. Lewis and M. F. Garbauskas, *Inorg. Chem.*, 1985, **24**, 363; (*i*) A. A. Pinkerton, D. Schwarzenbach, L. G. Hubert-Pfalzgraf and J. G. Riess, *Inorg. Chem.*, 1976, **15**, 1196.

6 (*a*) F. Akagi, Y. Ishida, T. Matsuo and H. Kawaguchi, *Dalton Trans.*, 2011, **40**, 2375; (*b*) F. Marchetti, G. Pampaloni and S. Zacchini, *Polyhedron*, 2009, **28**, 1235; (*c*) F. Marchetti, G. Pampaloni and S. Zacchini, *Dalton Trans.*, 2009, 8096; (*d*) F. Marchetti, G. Pampaloni and S. Zacchini, *Dalton Trans.*, 2008, 7026; (*e*) F. Preuss, G. Lambing and S. Müller-Becker, *Z. Anorg. Allg. Chem.*, 1994, **620**, 1812;

(*f*) A. Antiñolo, A. Otero, F. Urbanos, S. Garcia-Blanco, S. Martinez-Carrera and J. Sanz-Aparicio, *J. Organomet. Chem.*, 1988, **350**, 25; (*g*) L. R. Chamberlain, I. P. Rothwell and J. C. Huffman, *Inorg. Chem.*, 1984, **23**, 2575; (*h*) K. C. Malhotra, U. K. Banerjee and S. H. Chaudhry, *J. Ind. Chem.*, 1980, **57**, 868.

7 A. Dimitrov, S. Wuttke, S. Troyanov and E. Kemnitz, *Angew. Chem., Int. Ed.*, 2008, **47**, 190.

8 S. K. Ruediger, U. Groβ, M. Feist, H. A. Prescott, S. C. Shekar, S. I. Troyanov and E. Kemnitz, *J. Mater. Chem.*, 2005, **15**, 588.

9 M. Schormann, S. P. Varkey, H. W. Roesky and M. Noltemeyer, *J. Organomet. Chem.*, 2001, **621**, 310.

10 (*a*) M. H. Chisholm, J. C. Huffman and R. L. Kelly, *J. Am. Chem. Soc.*, 1979, **101**, 7100; (*b*) M. H. Crisholm, D. L. Clark and J. C. Huffman, *Polyhedron*, 1985, **7**, 1203.

11 M. H. Chisholm, D. L. Clark, R. J. Errington, K. Folting and J. C. Huffman, *Inorg. Chem.*, 1988, **27**, 2071.

12 C. Rennekamp, H. Wessel, H. W. Roesky, P. Müller, H.-G. Schmidt, M. Noltemeyer, I. Usón and A. R. Barron, *Inorg. Chem.*, 1999, **38**, 5235.

13 (*a*) Yu. A. Buslaev, Yu. V. Kokunov and V. A. Bochkareva, *Russ. J. Inorg. Chem.*, 1971, **16**, 2611; (*b*) A. Dimitrov, S. Seidel and K. Seppelt, *Eur. J. Inorg. Chem.*, 1999, 95.

14 R. Latham and R. S. Drago, *Inorg. Chem.*, 1964, **3**, 291.

15 A. M. Noble and J. M. Winfield, *J. Chem. Soc. A*, 1970, 501.

16 (*a*) R. Bini, C. Chiappe, F. Marchetti, G. Pampaloni and S. Zacchini, *Inorg. Chem.*, 2010, **49**, 339; (*b*) F. Marchetti, G. Pampaloni and S. Zacchini, *J. Fluorine Chem.*, 2010, **131**, 21; (*c*) F. Marchetti, G. Pampaloni and S. Zacchini, *Dalton Trans.*, 2009, 6759.

17 Yu. V. Kukunov, M. P. Gustyakova, V. A. Bochkareva, Yu. D. Chubar and Yu. A. Buslaev, *Sov. J. Coord. Chem.*, 1981, **7**, 354.

18 (*a*) Yu. A. Buslaev, Yu. V. Kokunov, S. M. Kremer and V. A. Shcherbakov, *Bull. Acad. Sci. USSR, Inorg. Mater.*, 1967, **3**, 1242; (*b*) Yu. A. Buslaev, Yu. V. Kokunov, S. M. Kremer and V. A. Shcherbakov, *Bull. Acad. Sci. USSR, Inorg. Mater.*, 1967, **3**, 1314; (*c*) M. Schönherr, *Z. Chem.*, 1976, **16**, 374.

19 F. P. Gortsema and R. Didchenko, *Inorg. Chem.*, 1965, **4**, 182.

20 J. C. Fuggle, D. W. A. Sharp and J. M. Winfield, *J. Chem. Soc.*, 1972, 1766.

21 The pentafluorides of niobium(v) and tantalum(v) (**1a,b**) have tetranuclear structure in the solid state. A. F. Wells, *Structural Inorganic Chemistry*, Clarendon Press, Oxford, 5th edn, 1993 and ref. 22 For sake of simplicity, the empirical formulas may be used throughout the present paper for **1a,b** and for their alkoxide derivatives.

22 C. G. Barrachlough, D. C. Bradley, J. Lewis and J. M. Thomas, *J. Chem. Soc.*, 1961, 2601.

23 A. J. Edwards, *J. Chem. Soc.*, 1964, 3714.

24 F. Marchetti, G. Pampaloni and S. Zacchini, *Inorg. Chem.*, 2008, **47**, 365.

25 (*a*) C. J. Cramer, *Essentials of Computational Chemistry*, 2nd edn, Wiley, Chichester, 2004; (*b*) F. Jensen, *Introduction to Computational Chemistry*, 2nd edn, Wiley, Chichester, 2007.

26 Cryoscopy measurements on presumed $[MF_2(OEt)_3]_n$ compounds in benzene gave $n = 2.5$ for M = Nb and $n = 2.4$ for M = Ta, see ref. 17.

27 M. G. B. Drew and J. D. Wilkins, *Inorg. Nucl. Chem. Lett.*, 1974, **10**, 549.

28 (*a*) A. Jutand, *Eur. J. Inorg. Chem.*, 2003, 2017; (*b*) W. J. Geary, *Coord. Chem. Rev.*, 1971, **7**, 81.

29 G. M. Sheldrick, *SADABS, Program for empirical absorption correction*, University of Göttingen, Göttingen, Germany, 1996.

30 G. M. Sheldrick, *SHELX97, Program for crystal structure determination*, University of Göttingen, Göttingen, Germany, 1997.

31 Y. Zhao and D. G. Truhlar, *Theor. Chem. Acc.*, 2008, **120**, 215.

32 (*a*) A. D. McLean and G. S. Chandler, *J. Chem. Phys.*, 1980, **72**, 5639; (*b*) L. E. Roy, P. J. Hay and R. L. Martin, *J. Chem. Theory Comput.*, 2008, **4**, 1029.

33 (*a*) V. Barone and M. Cossi, *J. Phys. Chem. A*, 1998, **102**, 1995; (*b*) M. Cossi, N. Rega, G. Scalmani and V. Barone, *J. Comput. Chem.*, 2003, 669.

34 M. J. Frisch, G. W. Trucks, H. B. Schlegel, G. E. Scuseria, M. A. Robb, J. R. Cheeseman, J. A. Montgomery Jr., T. Vreven, K. N. Kudin, J. C. Burant, J. M. Millam, S. S. Iyengar, J. Tomasi, V. Barone, B. Mennucci, M. Cossi, G. Scalmani, N. Rega, G. A. Petersson, H. Nakatsuji, M. Hada, M. Ehara, K. Toyota, R. Fukuda, J. Hasegawa, M. Ishida, T. Nakajima, Y. Honda, O. Kitao, H. Nakai, M. Klene, X. Li, J. E. Knox, H. P. Hratchian, J. B. Cross, C. Adamo, J. Jaramillo, R. Gomperts, R. E. Stratmann, O. Yazyev, A. J. Austin, R. Cammi, C. Pomelli, J. W. Ochterski, P. Y. Ayala, K. Morokuma, G. A. Voth, P. Salvador, J. J. Dannenberg, V. G. Zakrzewski, S. Dapprich, A. D. Daniels, M. C. Strain, O. Farkas, D. K. Malick, A. D. Rabuck, K. Raghavachari, J. B. Foresman, J. V. Ortiz, Q. Cui, A. G. Baboul, S. Clifford, J. Cioslowski, B. B. Stefanov, G. Liu, A. Liashenko, P. Piskorz, I. Komaromi, R. L. Martin, D. J. Fox, T. Keith, M. A. Al-Laham, C. Y. Peng, A. Nanayakkara, M. Challacombe, P. M. W. Gill, B. Johnson, W. Chen, M. W. Wong, C. Gonzalez and J. A. Pople, *GAUSSIAN03 (Revision A.1)*, Gaussian, Inc., Pittsburgh, 2003.